Dispersion of Small Suspended Particles in a Wave Boundary Layer

CHIANG C. MEI AND CHIMIN CHIAN

R. M. Parsons Laboratory, Department of Civil and Environmental Engineering, Massachusetts Institute of Technology, Cambridge, Massachusetts

(Manuscript received 2 August 1993, in final form 15 February 1994)

ABSTRACT

The dispersion of heavy suspensions in a wave boundary layer over a nonerodible bed is examined theoretically. Focusing attention on the horizontal variation of the ambient wave pattern, an effective convection–diffusion equation is derived by extending the theory of homogenization (multiple scales). For the model based on constant eddy diffusivities, the effective velocity of horizontal convection and shear-enhanced dispersion tensor are derived explicitly for very general wave patterns over a horizontal seabed. The convection velocity is found to be related to Eulerian streaming inside the boundary layer, weighted by the mean concentration profile. Particular examples are examined for the release of a finite cloud of suspension beneath gravity waves at various locations relative to the wave pattern.

1. Introduction

Taylor's (1953) pioneering work on dispersion in a steady flow through a tube has been extended to oscillatory flows by many authors. For laminar flows, the case of an oscillatory axial flow in a uniform tube was first treated by Aris (1960) by the moment method. Theories for the same geometry have been advanced by Chatwin (1975) and Watson (1983) by other methods. Pedley and Kamm (1988) and Sharp et al. (1991) have analyzed the additional effects of transverse circulation, which exist in winding blood vessels. For three-dimensional flows, Dill and Brenner (1982) have developed a formal theory for dispersion in an oscillatory flow through a periodic porous medium.

Dispersion in oscillatory turbulent flows is a vital problem related to coastal pollution. Bowden (1965) gave the first theory for a horizontally uniform tidal current based on constant and depth-dependent vertical eddy viscosities. To simulate homogeneous estuary flows, Holly et al. (1970) analyzed the period dependency of the dispersion coefficient in an oscillatory two-dimensional channel flow with a linear velocity profile. The similar problem of dispersion in an alternating current in a channel was also studied by Fukuoka (1974). The effects of width and depth of an estuary have been studied by Smith (1982) with a special focus on the near field of the contaminant source. In these works the basic flow is spatially uniform and the suspension is passive and neutrally buoyant. For spatially nonuniform oscillating flows, Zimmerman (1986) and Geyer and Signal (1992) have reviewed the dispersion in tides.

Dispersion of heavy particles is of interest not only to the physical process of sand or silt transport, but also to biological processes in the sea. The convective and diffusive transport by waves and current in coastal waters is important to the birth and growth of planktonic larvae (Denny 1988). Sayre (1968, 1969) and Sumer (1974) investigated steady uniform open channel flows relevant to river morphology. For oscillatory flows, Yasuda (1989) presented a theory on the transient process of dispersion in an oscillating, horizontally uniform current with a Stokes boundary layer. He also studied the initial phase of dispersion of particles released from the water surface. The important effect of the fall velocity of the particles on dispersion in oscillatory flows and on both dispersion and convection in steady flows was recognized by these authors. There have also been numerical models that solve the regular diffusion equation with finite fall velocity for transport of sediments in turbulent channel flows (e.g., Kerssens et al. 1977). In all of these studies, the flow is assumed to be unaffected by the particles. Noh and Fernando (1991), however, have accounted for the effect of sediments on the turbulent energy in their study of the vertical diffusion of sediments in a horizontally uniform flow and the formation of a lutocline.

In coastal regions, transport of suspended particles by waves is most effective near the bottom where there is an oscillatory boundary layer. The dynamics of the fluid flow itself in the boundary layer has been studied extensively for laminar or pseudolaminar flows. In addition to the oscillatory velocity field, there is the steady

Corresponding author address: Prof. Chiang C. Mei, Department of Civil and Environmental Engineering, Ralph M. Parsons Laboratory Room 48-413, Massachusetts Institute of Technology, Cambridge, MA 02139.
E-mail: ccmei@mit.edu

Eulerian streaming induced by Reynolds stresses. The corresponding Lagrangian drift can be used to infer the motion of marked fluid particles (or dye). Such information may be found in Longuet-Higgins (1953), Hunt and Johns (1963), and Mei (1983). Models for turbulent wave boundary layers based on depth-dependent eddy viscosities have also been given by Kajiura (1968) and Grant and Madsen (1979) with the primary view of calculating the friction factor and its effects on wave damping, and by Longuet-Higgins (1958), Johns (1970), and Trowbridge and Madsen (1984) for mass transport.

In this paper we shall examine the long-time dispersion of suspended particles in a wave boundary layer with significant variations in the horizontal plane. The basic flow is therefore three-dimensional. Attention will be focused on small amplitude waves without ambient current so that the mean Eulerian streaming induced by waves is weaker than wave oscillations. The bed is assumed to be nonerodible or effectively nonerodible, and the particle cloud is released from an external source. Thus, the theory is intended for the spreading of fine contaminants or sewage effluent that is dumped near the seabed, or to tiny clay particles, initially brought to suspension during a transient period of relatively strong storm waves. With sufficiently small fall velocity, these particles can be expected to remain in suspension throughout most of the wave cycle. There can of course be larger or heavier particles, as well as highly erodible beds where entrainment and resuspension are important during a significant part of a wave cycle; but these bed processes involve additional uncertainties. Although their inclusion in the present theory is in principle possible by adding empirical hypotheses, they are not considered here.

We shall make use of the fact that the timescale of horizontal diffusion is expected to be much longer than the wave period, and employ the method of multiple scales to find the effective convective–diffusion equation and the dispersivity (effective diffusivity) tensor. The latter is the correlation between fluctuations of velocity and sediment concentration, and can be calculated once a turbulence model is chosen. Our mathematical procedure is a modification of the homogenization theory (Bensoussan et al. 1978) that has been applied to the dispersion of a solute in a spatially periodic porous medium (Rubinstein and Mauri 1986; Mauri 1991; Mei 1991, 1992). In this paper we shall make the simplifying assumption of constant eddy diffusivities to obtain analytical results that do not differ substantially from a numerical theory based on an empirical model of depth-dependent eddy diffusivities. General and explicit formulas will be obtained for the effective diffusion equation, the effective convection velocity, and dispersivity tensor for waves of any spatial pattern. Detailed examples will be worked out for gravity waves. After calculating the dispersivity tensor, which is in general space dependent, examples of diffusion from a local source will be studied. The dependence of the convective diffusion on the wave pattern and the source location will be examined.

2. Basic assumptions and effective convection–diffusion equations

While in general a heavy suspended particle need not follow the moving fluid in its surroundings, for sufficiently small particles the velocity difference can be negligible. By comparing the particle inertia with the fluid drag force, Bagnold (1951) has estimated that the difference in velocity between a spherical particle and its surrounding fluid will be reduced from its initial value Δu by half within the following relaxation time

$$\tau = \frac{8a}{3C_D}\frac{\rho_s}{\rho\,\Delta u}, \tag{2.1}$$

where ρ denotes water density, ρ_s the sphere density, a the sphere radius, and C_D the drag coefficient. The velocities are the ensemble averages over turbulent fluctuations, and the fluid drag on the particle is assumed to be quadratic in Δu. For wave motion of characteristic frequency ω, the ratio of timescales is

$$\omega\tau = \frac{8a}{3C_D}\frac{\rho_s}{\rho}\frac{\omega}{\Delta u}. \tag{2.2}$$

Taking for estimation $a = 0.01$ cm which is typical of fine sand or silt, $\Delta u = 10$ cm s^{-1}, $\rho_s/\rho = 2.5$, $C_D = 1$, and $\omega = 1 \sim 0.01$ rad s^{-1} (typical of surface and internal waves), we get $\omega\tau = 0.67 \times 10^{-2} \sim 0.67 \times 10^{-4}$ which is very small. Therefore such a small suspended particle acquires the ensemble-mean velocity of the neighboring fluid almost instantly. For still smaller particles, Stokes drag formula may be used to define the relaxation time similarly (Saffman 1962),

$$\omega\tau = \frac{2}{9}\frac{\omega}{\nu}\frac{a^2\rho_s}{\rho}, \tag{2.3}$$

which is also negligibly small.[1]

Here we shall assume the particles to be small enough so that the particle velocity due to fluid oscillation is essentially equal to the ensemble mean velocity of the local fluid. The fall velocity, however, is not ignored as it is unrelated to wave motion and nonzero even if the ambient fluid is completely calm.

For modeling turbulent wave boundary layers in the sea, there have been numerical and semi-empirical

[1] Lumley (1978) also gave a criterion for a particle to be inertia-free relative to turbulent fluctuations, if the particle size is much smaller than the Kolmogorov length $l_k = (\nu^3 l/u'^3)^{1/4}$, where l is the eddy size and u' the velocity scale of turbulent fluctuations. Estimating the boundary layer thickness $\delta = O(\nu_e/\omega)^{1/2}$ and $u' = (0.1)\omega A$ in a wave of amplitude A, it can be shown for waves with typical values $\omega = 1$ rad s^{-1} and $\omega A = 0.1$ m s^{-1}, $\nu_e = 10^{-3}$ m^2 s^{-1}, that $l_k = 0.04$ cm. Thus, particles much smaller than 40 μm are inertia free even relative to the turbulent fluctuations.

models of various degrees of complexity (eddy viscosity, mixing length, k–ϵ, second-order closure, etc.). Despite the differences in details, models of time-independent eddy viscosity, depth-dependent or even constant, do not give substantially different predictions for the ensemble-averaged velocity profile. These models have been extensively surveyed by Sleath (1990). In this paper, we shall adopt the simplest model of constant eddy diffusivity model, a common approximation in oceanography, in order to facilitate analytical results. In addition, no distinction of horizontal and vertical diffusivities will be made for lack of reliable empirical information. In a parallel study, we have employed a depth-dependent eddy diffusivity proposed by Lundgren (1972) and reexamined the present problem. Similar results have been obtained after considerable numerical work (Chian 1993). We note that some experiments suggest that the diffusivity depends on time as well, and this dependence may alter the flow qualitatively (Trowbridge and Madsen 1984). However, experimental data are not comprehensive enough for constructing a reliable model.

Let C denote the volume concentration, $-w_0$ the fall velocity of the suspended particles, and D the eddy mass diffusivity. The diffusion equation for the concentration C of a very dilute sediment cloud can be approximated by

$$\frac{\partial C}{\partial t} + \frac{\partial u_i C}{\partial x_i} + \frac{\partial}{\partial z}[(-w_0 + w)C] = D\left(\frac{\partial^2 C}{\partial x_i \partial x_i} + \frac{\partial^2 C}{\partial z^2}\right), \quad (2.4)$$

where $i = 1, 2$ with $(x_1, x_2) \equiv (x, y)$ and $(u_1, u_2) \equiv (u, v)$ representing the horizontal coordinates and the fluid velocity components. The vertical coordinate and velocity component are denoted by z and w. Equation (2.4) is useful when C is sufficiently small so that the presence of the particles does not materially alter the fluid flow. (Two measures of the effects of non-neutrally buoyant suspensions in the supporting fluid are the effective viscosity and buoyancy force. Both are negligible for $C < 10^{-3}$, say.)

At the sea bottom the boundary condition for C is the least certain if the bed surface is erodible, and various assumptions have been made in the literature of sediment transport. In a uniform and steady flow, the concentration at the bed surface cannot be determined theoretically and must be regarded as a measured quantity. For steady but nonuniform flows, Sayre (1969) proposed the following empirical relation:

$$D\frac{\partial C}{\partial z} + (1 - \alpha)w_0 C + W = 0, \quad (2.5)$$

to model resuspension and deposition, where α is the bed absorbency coefficient representing the probability that a particle settling to the bed is deposited there and W the average rate of local entrainment. Direct measurements of α and W are obviously difficult and none is known to have been made. For wave boundary layers it has also been proposed that the concentration flux at the bed is an empirical (pickup) function of time, representing the rate of resuspension (Staub et al. 1984). Smith (1977) introduced a criterion that the bed concentration is proportional to the difference between bed shear stress and the critical shear stress at which the sediments begin to move. The coefficient of proportionality must again be found empirically but reliable information is scarce. In addition, the criterion is only appropriate for an erodible bed that has an unlimited supply of sediments so that the bed concentration is in principle fixed. We shall consider only those particles brought into suspension by causes external to the flow in consideration, for example, by human dumping, and which remain in suspension by turbulence and the small fall velocity. The bed is otherwise nonerodible under the sufficiently small amplitude waves. Thus, the wave-induced flow must be sufficiently strong so that particles placed in suspension by an external source remain in suspension, but sufficiently weak so that local resuspension from the bottom does not occur. Accordingly, we shall take the simplest assumption that there is no exchange of particles with the seabed

$$D\frac{\partial C}{\partial z} + w_0 C = 0, \quad z = 0. \quad (2.6)$$

This no-flux condition[2] has been used by Yasuda (1989) for dispersion in tidal flows.

Outside the boundary layer we assume

$$C = 0, \quad z \to \infty. \quad (2.7)$$

In addition, the initial horizontal distribution of the depth-averaged concentration is prescribed in some source area. Thus, the physical problem is to seek the long-time diffusion of a particle cloud from a localized source.

In the present problem there are several characteristic length scales in the vertical direction. The first is the thickness of a steady concentration layer due to the balance of downward sedimentation by gravity and vertical diffusion,

$$d \sim \frac{D}{w_0}. \quad (2.8)$$

Associated with fluid oscillations at frequency ω there are two additional vertical length scales; that is, the oscillatory boundary layer thicknesses

[2] A mathematically similar but physically different boundary condition applies for diffusion in seepage flows involving chemical reactions (Shapiro and Brenner 1988; Mauri 1991), where w_0 corresponds to the chemical reaction rate.

$$\delta \sim \sqrt{2\nu_e/\omega} \quad \text{and} \quad \delta_D \sim \sqrt{2D/\omega} \tag{2.9}$$

corresponding, respectively, to oscillatory momentum and mass diffusion. For generality, all three scales are assumed to be comparable; that is,

$$\frac{\delta}{d} \leqslant O(1) \tag{2.10}$$

and

$$\mathrm{Sc} = \frac{\nu_e}{D} \sim \left(\frac{\delta}{\delta_D}\right)^2 = O(1), \tag{2.11}$$

where Sc is the Schmidt number. Invoking Reynolds analogy, $D = \nu_e$, and using $\nu_e \sim \kappa u_* \delta$ as an estimate, where $\kappa = 0.4$ is von Kármán's constant (Kajiura 1968), $d \sim \kappa u_* \delta / w_0$; (2.10) is seen to be consistent with (2.7).

We now consider small amplitude oscillations of high enough frequency so that both wave steepness, kA (k = wavenumber) and the ratio of the oscillatory boundary layer thickness to the wavelength, $k\delta$, are small; that is,

$$\epsilon = kA \ll 1, \quad \beta = k\delta \ll 1. \tag{2.12a,b}$$

Assuming for generality that $\epsilon = O(\beta)$, we may introduce the following normalization:

$$x_i^* = kx_i, \quad z^* = z/\delta, \quad u_i^* = u_i/\omega A,$$
$$w^* = w/k\delta\omega A, \quad t^* = \omega t. \tag{2.13}$$

The diffusion equation (2.4) is rescaled to become

$$\frac{\partial C^*}{\partial t^*} + \epsilon \frac{\partial u_i^* C^*}{\partial x_i^*} + \frac{\partial}{\partial z^*}[(-\mathrm{Pe} + \epsilon w^*)C^*] = \beta^2 \frac{\partial^2 C^*}{\partial x_i^* \partial x_i^*} + \frac{\partial^2 C^*}{\partial z_*^2}, \tag{2.14}$$

where $\mathrm{Pe} = w_0\delta/D$ is a Peclét number based on the fall velocity. Equations (2.6) and (2.8) remain unchanged. Having identified the orders we return to the dimensional form (2.4) by inserting an ordering parameter ϵ as follows:

$$\frac{\partial C}{\partial t} + \epsilon \frac{\partial u_i C}{\partial x_i} + \frac{\partial}{\partial z}[(-w_0 + \epsilon w)C] = D\left(\epsilon^2 \frac{\partial^2 C}{\partial x_i \partial x_i} + \frac{\partial^2 C}{\partial z^2}\right). \tag{2.4′}$$

Clearly, there are two distinct timescales in the diffusion process, one for vertical diffusion across the boundary layer, $O(\omega^{-1}) = O(\delta^2/D)$, which is the same as a wave period, and one for horizontal diffusion across a wavelength, $O(1/k^2D)$. The ratio between the two is $O(k^2\delta^2) = O(\beta^2)$. In most natural flows of interest β is much smaller than ϵ. We shall, however, make a generous assumption that $O(\epsilon) = O(\beta)$. A consequence is that the horizontal diffusion is retained in the final diffusion equation, as will be shown. If $\beta \ll \epsilon$, the same term can be ignored. Under the assumption $\epsilon = O(\beta)$ we shall introduce multiple-scale coordinates for time: t and $T = \epsilon^2 t$. The velocity and concentration are expanded as follows:

$$u_i = u_i^{(1)} + \epsilon u_i^{(2)} + O(\epsilon^2)$$
$$w = w^{(1)} + \epsilon w^{(2)} + O(\epsilon^3)$$
$$C = C^{(0)} + \epsilon C^{(1)} + \epsilon^2 C^{(2)} + O(\epsilon^3), \tag{2.15}$$

where $u_i^{(n)}$ and $w^{(n)}$ are functions of x_i, z, and t and $C^{(n)} = C^{(n)}(x_i, z, t, T)$. At leading order $C^{(0)}(x_i, z, T)$ is expected to represent the period average and depends only on T. The diffusion equation at $O(1)$ is a homogeneous differential equation in z

$$-w_0 \frac{\partial C^{(0)}}{\partial z} = D \frac{\partial^2 C^{(0)}}{\partial z^2}, \quad 0 < z < \infty. \tag{2.16}$$

The homogeneous boundary conditions are

$$w_0 C^{(0)} + D \frac{\partial C^{(0)}}{\partial z} = 0, \quad z = 0 \tag{2.17}$$

$$C^{(0)} = 0, \quad z \to \infty. \tag{2.18}$$

Thus, a nontrivial solution exists

$$C^{(0)} = \hat{C}(x_i, T)F(z), \tag{2.19}$$

where

$$F(z) = \exp\left(-\frac{w_0 z}{D}\right), \tag{2.20}$$

and $\hat{C}$ is the concentration at the seabed. Recall that in the classical case of uniform and steady flows, $\hat{C}$ is indeterminate theoretically. Here nonuniformity and nonstationarity will allow us to determine $\hat{C}$.

At $O(\epsilon)$, $C^{(1)}$ represents the perturbation due to the oscillating velocity field and satisfies

$$\frac{\partial C^{(1)}}{\partial t} - w_0 \frac{\partial C^{(1)}}{\partial z} - D \frac{\partial^2 C^{(1)}}{\partial z^2} = -\frac{\partial (u_i^{(1)} C^{(0)})}{\partial x_i} - \frac{\partial (w^{(1)} C^{(0)})}{\partial z} \tag{2.21}$$

and the boundary conditions

$$w_0 C^{(1)} + D \frac{\partial C^{(1)}}{\partial z} = 0, \quad z = 0 \tag{2.22}$$

$$C^{(1)} = 0, \quad z \to \infty. \tag{2.23}$$

At $O(\epsilon^2)$, $C^{(2)}$ satisfies

$$\frac{\partial C^{(2)}}{\partial t} - w_0 \frac{\partial C^{(2)}}{\partial z} - D \frac{\partial^2 C^{(2)}}{\partial z^2} = -\frac{\partial C^{(0)}}{\partial T} - \frac{\partial u_i^{(1)} C^{(1)}}{\partial x_i} - \frac{\partial w^{(1)} C^{(1)}}{\partial z} - \frac{\partial u_i^{(2)} C^{(0)}}{\partial x_i} - \frac{\partial w^{(2)} C^{(0)}}{\partial z} + D \frac{\partial^2 C^{(0)}}{\partial x_j \partial x_j} \tag{2.24}$$

and the boundary conditions

$$w_0 C^{(2)} + D\frac{\partial C^{(2)}}{\partial z} = 0, \quad z = 0 \tag{2.25}$$

$$C^{(2)} = 0, \quad z \to \infty. \tag{2.26}$$

Our interest is in slow diffusion at leading order, and attention will be focused on the governing equation for the factor $\hat{C}(x_i, T)$, defined by (2.19).

Let us assume that the velocity field at leading order $(u_i^{(1)}, w^{(1)})$ is simple harmonic in time with the frequency ω. All forcing terms on the rhs of (2.21) are then simple harmonic in the fast time t. Let the period average (time average with respect to a wave period) of $C^{(1)}$ be denoted by $\bar{C}^{(1)}$. Then $\bar{C}^{(1)}$ satisfies the homogeneous equation (2.16) also and the homogeneous boundary conditions (2.22) and (2.23). Without loss of generality we shall take $\bar{C}^{(1)} = 0$ so that $C^{(1)}$, which corresponds to the departure from the zeroth-order mean $C^{(0)}$, consists only of first harmonic fluctuations:

$$C^{(1)} = \Re(C_{11} e^{-i\omega t}), \tag{2.27}$$

where $C_{11} = C_{11}(x_i, z, T)$ and $\Re$ denotes the real part of its argument (for later use, $\Im$ denotes the imaginary part). Averaging (2.24), (2.25), and (2.26) over the wave period, we find that the time average $\bar{C}^{(2)}$ of $C^{(2)}$ satisfies an inhomogeneous differential equation similar to (2.16), and the boundary conditions (2.17) and (2.18). Solution of the inhomogeneous boundary value problem for $\bar{C}^{(2)}$ leads to

$$\frac{\partial}{\partial T}\langle C^{(0)}\rangle + \frac{\partial}{\partial x_i}\langle \bar{u}_i^{(2)} C^{(0)}\rangle = -\frac{\partial}{\partial x_i}\langle \overline{u_i^{(1)} C^{(1)}}\rangle + D\frac{\partial^2 \langle C^{(0)}\rangle}{\partial x_j \partial x_j}. \tag{2.28}$$

Mathematically, this is just the Fredholm alternative or solvability condition for an inhomogeneous boundary value problem, which possesses a nontrivial homogeneous solution (here $C^{(0)}$). It follows by using (2.19) that

$$\frac{\partial \hat{C}}{\partial T}\langle F\rangle + \frac{\partial}{\partial x_i}[\langle \bar{u}_i^{(2)} F\rangle \hat{C}] = -\frac{\partial}{\partial x_i}\langle \overline{u_i^{(1)} C^{(1)}}\rangle + D\frac{\partial^2}{\partial x_j \partial x_j}[\hat{C}\langle F\rangle], \tag{2.29}$$

where $\langle f\rangle$ represents depth integration of f from $z = 0$ to $z = \infty$. This gives the effective convection–diffusion equation for $\hat{C}$.

The present scheme is a modification of the usual method of homogenization, which has been applied to dispersion in porous media with a spatially periodic structure on the microscale (Rubinstein and Mauri 1986; Mauri 1991; Mei 1991, 1992). We have simply modified it for a time-periodic problem here.

In existing studies of steady flows, the convection term is contributed by the leading-order velocity of the steady flow. As is recalled in the next section, $\bar{u}^{(2)}$ represents the second-order Eulerian streaming induced by Reynolds stresses, hence the convective inertia. Therefore the effective convection velocity in the horizontal plane is essentially the weighted depth average of $\bar{u}_i^{(2)}$ with the weight $F(z)$. Now the first term on the right-hand side of (2.29) is the result of convection by the first-order oscillatory velocity, leading to an apparent diffusion analogous to Taylor dispersion. The last term represents horizontal diffusion due directly to turbulence.

In the next sections we shall recall the known velocity field $u_i^{(1)}$, $\bar{u}_i^{(2)}$ from past works; $C^{(1)}$ is next solved and combined with $u_i^{(1)}$ for computing the correlations. Specific examples for the release of a particle cloud then follow.

3. Velocity field in the wave boundary layer

We restrict our attention to surface or internal gravity waves whose length and periods are short enough so that the earth rotation is negligible. For small amplitudes linearized inviscid theory can be used to compute the flow velocity above the seabed. To ensure no slip at the bed, an oscillatory boundary layer of the Stokes type must be added. At second order in wave steepness, convective inertia in the boundary layer induces a mean shear stress that drives a second-order mean current (Eulerian streaming). For a horizontal seabed and constant eddy viscosity, both first-order oscillation $u^{(1)}$ and second-order mean drift $\bar{u}^{(2)}$ can be inferred from Hunt and Johns (1963), see also Mei (1983). Let the inviscid wave motion just above the boundary layer be simple harmonic in time to leading order

$$U_i = \Re(U_{0i} e^{-i\omega t}), \tag{3.1}$$

where $U_{0i} = U_{0i}(x_j)$ is the spatial amplitude of U_i. For constant eddy viscosity, a straightforward power series expansion in terms of $\epsilon = kA$ gives at first order the Stokes solution

$$u_i^{(1)} = \Re[U_{0i} F_1(z) e^{-i\omega t}],$$
$$w^{(1)} = \Re\left[\frac{1}{\alpha}\frac{\partial U_{0i}}{\partial x_i} F_w(z) e^{-i\omega t}\right] \tag{3.2}$$

with

$$F_1(z) = 1 - e^{-\alpha z}, \quad F_w(z) = 1 - e^{-\alpha z} - \alpha z, \tag{3.3a,b}$$

and

$$\alpha = \frac{1 - i}{\delta}. \tag{3.4}$$

At second order we only need the time average with respect to period $2\pi/\omega$,

$$\bar{u}^{(2)}(x_i, z) = -\frac{1}{\omega}\Re\left[F_2 U_0 \frac{\partial U_0^*}{\partial x} + F_3 V_0 \frac{\partial U_0^*}{\partial y} + F_4 U_0 \frac{\partial V_0^*}{\partial y}\right]$$

$$\bar{v}^{(2)}(x_i, z) = -\frac{1}{\omega}\Re\left[F_2 V_0 \frac{\partial V_0^*}{\partial y} + F_3 U_0 \frac{\partial V_0^*}{\partial x} + F_4 V_0 \frac{\partial U_0^*}{\partial x}\right], \quad (3.5)$$

with

$$F_2 = -\frac{1}{2}(1 - 3i)e^{(-1+i)\xi} - \frac{1+i}{4}e^{-2\xi} + \frac{1}{2}(1+i)\xi e^{(-1+i)\xi} + \frac{3}{4}(1-i) \quad (3.6a)$$

$$F_3 = \frac{1}{2}ie^{(-1+i)\xi} - \frac{i}{2}e^{-(1+i)\xi} - \frac{1}{4}e^{-2\xi} + \frac{1}{4} \quad (3.6b)$$

$$F_4 = -\frac{1}{2}(1 - 2i)e^{(-1+i)\xi} + \frac{1+i}{2}\xi e^{-(1-i)\xi} - \frac{i}{4}e^{-2\xi} + \frac{1}{4}(2 - 3i), \quad (3.6c)$$

where $\xi = z/\delta$.

4. The effective dispersion equation

a. Derivation

At first order, the concentration fluctuation $C^{(1)}$, formally given by (2.27), must satisfy (2.21). By substituting (3.2) and (2.19) into the right-hand side of (2.21) and extracting the coefficient of the first harmonic part, we get

$$\frac{d^2C_{11}}{dz^2} + \frac{1}{d}\frac{dC_{11}}{dz} + \frac{i\omega}{D}C_{11} = G_1(z) \quad (4.1)$$

with

$$G_1 = \frac{1}{D}\left[\left(U_{0i}\frac{\partial \hat{C}}{\partial x_i}\right)e^{-z/d}F_1(z) - \frac{\hat{C}}{\alpha d}\left(\frac{\partial U_{0i}}{\partial x_i}\right)e^{-z/d}F_w(z)\right]. \quad (4.2)$$

The homogeneous solution to (4.1) is a linear combination of $e^{\beta_1 z}$ and $e^{\beta_2 z}$, where

$$\beta_{1,2} = -\frac{1}{2d}(1 + (1 + N^4)^{1/4}e^{-i\theta/2}) = -\frac{1}{2d}\left[1 \mp (1+N^4)^{1/4}\cos\frac{\theta}{2}\right] \mp \frac{i}{2d}(1+N^4)^{1/4}\sin\frac{\theta}{2} \quad (4.3)$$

with

$$N = 2d\left(\frac{\omega}{D}\right)^{1/2} = \frac{2\sqrt{2\mathrm{Sc}}}{\mathrm{Pe}}, \quad \mathrm{Pe} = \frac{w_0\delta}{D} = \frac{\delta}{d}, \quad (4.4)$$

where

$$\cos\theta = (1 + N^4)^{-1/2},$$

$$\text{and} \quad \cos\frac{\theta}{2} = \left[\frac{1}{2}(1 + \cos\theta)\right]^{1/2}. \quad (4.5)$$

It is easy to show that

$$(1 + N^4)^{1/4}\cos\frac{\theta}{2} = \left\{\frac{1}{2}[1 + (1 + N^4)^{1/2}]\right\}^{1/2} > 1 \quad (4.6)$$

so that

$$\Re(\beta_1) > 0 \quad \text{and} \quad \Re(\beta_2) < 0. \quad (4.7)$$

Thus, for boundedness at $z \sim \infty$, only $e^{\beta_2 z}$ is admissible as a homogeneous solution. By the standard method of variation of parameters, the inhomogeneous solution can be found. In usual homogenization analyses, the forcing terms and the resonance of the $O(\epsilon)$ problems are proportional to the gradient of the zeroth-order solution. From (4.1) and (4.2), the forcing terms of C_{11} involve both $\partial\hat{C}/\partial x_i$ and $\hat{C}$, hence the solution is

$$C_{11} = R_0 e^{\beta_2 z} + R_1 e^{-z/d} + R_2 e^{-(1/d+\alpha)z} + R_3 z e^{-z/d}, \quad (4.8)$$

where

$$R_0 = \frac{d}{1 + \beta_2 d}(\alpha R_2 - R_3)$$

$$R_1 = \frac{d^2}{D(1+\beta_1 d)(1+\beta_2 d)}\left\{U_{0j}\frac{\partial \hat{C}}{\partial x_j} + \left[\frac{2 + \beta_1 d + \beta_2 d}{(1+\beta_1 d)(1+\beta_2 d)} - \frac{1}{\alpha d}\right]\frac{\partial U_{0i}}{\partial x_i}\hat{C}\right\}$$

$$R_2 = -\frac{d^2}{D(1 + \beta_1 d + \alpha d)(1 + \beta_2 d + \alpha d)} \times \left(U_{0j}\frac{\partial \hat{C}}{\partial x_j} - \frac{1}{\alpha d}\frac{\partial U_{0i}}{\partial x_i}\hat{C}\right)$$

$$R_3 = \frac{d}{D(1+\beta_1 d)(1+\beta_2 d)}\frac{\partial U_{0i}}{\partial x_i}\hat{C}. \quad (4.9)$$

Thus, the concentration fluctuation $C^{(1)}$ is found in terms of $\hat{C}$ and its horizontal gradient. Equations (3.2), (3.5), and (2.27) may now be put in (2.29). After some algebra we get the effective diffusion equation for $\hat{C}$:

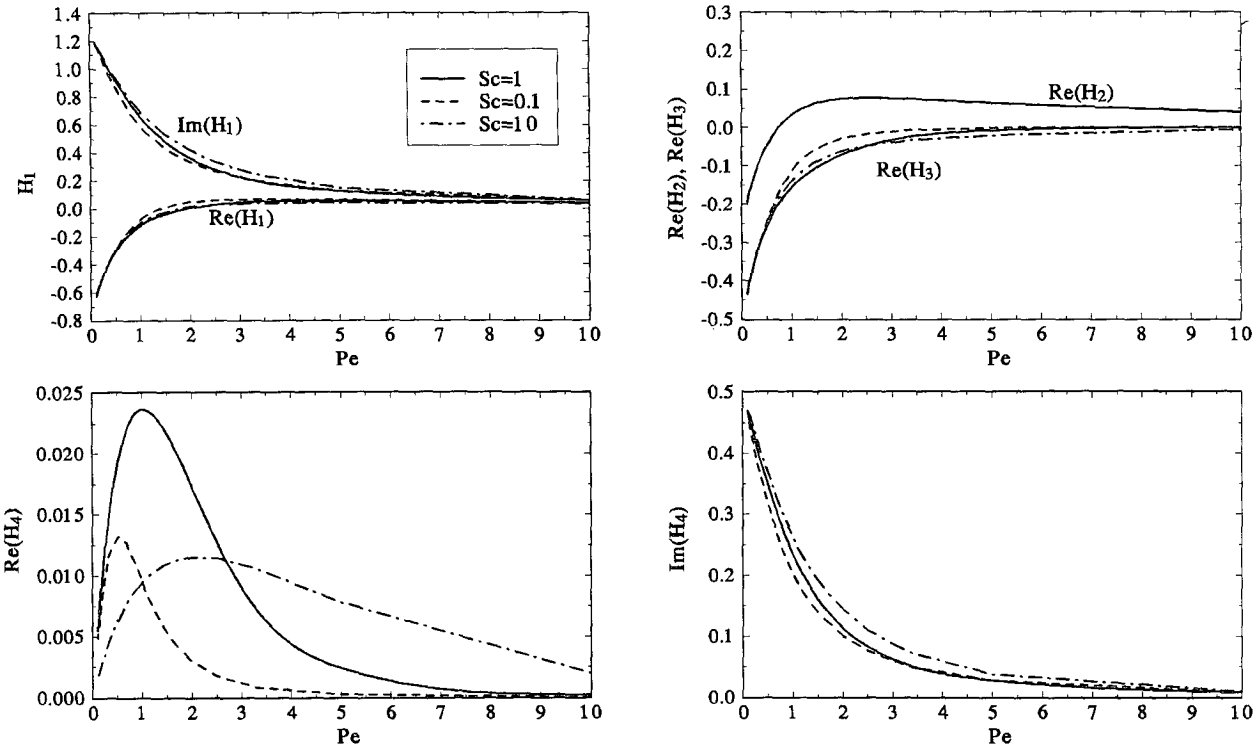

FIG. 1. Coefficients H_1, H_2, H_3, and H_4 as functions of Peclét number Pe for Schmidt number Sc = 0.1, 1, and 10. Note that H_2 is real and $\Im(H_3) = \Im(H_1)$.

$$\frac{\partial \hat{C}}{\partial T} + \frac{\partial}{\partial x_i}(\mathcal{U}_i \hat{C}) = D\frac{\partial^2 \hat{C}}{\partial x_j \partial x_j} + \frac{\partial}{\partial x_i}\left(E_{ij}\frac{\partial \hat{C}}{\partial x_j}\right), \tag{4.10a}$$

where

$$\mathcal{U} = \frac{1}{\omega}\Re\left(H_1 U_0 \frac{\partial U_0^*}{\partial x} + H_2 V_0 \frac{\partial U_0^*}{\partial y} + H_3 U_0 \frac{\partial V_0^*}{\partial y}\right)$$

$$\mathcal{V} = \frac{1}{\omega}\Re\left(H_1 V_0 \frac{\partial V_0^*}{\partial y} + H_2 U_0 \frac{\partial V_0^*}{\partial x} + H_3 V_0 \frac{\partial U_0^*}{\partial x}\right) \tag{4.10b}$$

$$E_{xx} = \Re\left[\frac{H_4}{\omega}|U_0|^2\right], \quad E_{xy} = \Re\left[\frac{H_4}{\omega}(U_0^* V_0)\right]$$

$$E_{yx} = \Re\left[\frac{H_4}{\omega}(U_0 V_0^*)\right], \quad E_{yy} = \Re\left[\frac{H_4}{\omega}|V_0|^2\right]. \tag{4.10c}$$

Here $\mathcal{U}$ and $\mathcal{V}$ are the components of weighted depth-average of Eulerian streaming (3.5) while the tensor E_{ij} arises from the correlation tensor $\langle u_i^{(1)} C^{(1)}\rangle$. The formulas deduced here are quite general for any small amplitude wave field as long as the first-order inviscid velocity U_0, V_0 in the tangential direction is known at the upper edge of the boundary layer. Expressions of the complex coefficients H_1, H_3, and H_4 and the real coefficient H_2 are given in the appendix and plotted as functions of Pe and Sc in Figs. 1a–d.

Introducing the flux vector $\mathcal{F}_i$ defined by

$$\mathcal{F}_i = \mathcal{U}_i \hat{C} - (E_{ij} + D\delta_{ij})\frac{\partial \hat{C}}{\partial x_j}, \tag{4.11}$$

we may write (4.10a) in conservation form

$$\frac{\partial \hat{C}}{\partial T} + \frac{\partial \mathcal{F}_i}{\partial x_i} = 0. \tag{4.12}$$

b. Coefficient tensor E_{ij}

Before presenting numerical results, some general comments are warranted. Because H_4 is complex, the tensor E_{ij}, which is not of thermodynamic origin, is in general not symmetric, that is, $E_{ij} \neq E_{ji}$; but one may rewrite E_{ij} as the sum of a symmetric and an antisymmetric part

$$E_{ij} = \mathcal{D}_{ij} + \mathcal{A}_{ij}, \tag{4.13}$$

where

$$\mathcal{D}_{ij} = \frac{1}{2}(E_{ij} + E_{ji}) = \mathcal{D}_{ji} \quad \text{and}$$

$$\mathcal{A}_{ij} = \frac{1}{2}(E_{ij} - E_{ji}) = -\mathcal{A}_{ji}. \tag{4.14}$$

Since

$$\mathcal{A}_{ij}\frac{\partial^2\hat{C}}{\partial x_i\partial x_j} = -\mathcal{A}_{ji}\frac{\partial^2\hat{C}}{\partial x_i\partial x_j} = 0, \qquad (4.15)$$

the antisymmetric part $\mathcal{A}_{ij}$ is not diffusive. The associated term in (4.10a) may be rewritten as

$$\frac{\partial}{\partial x_i}\left(\mathcal{A}_{ij}\frac{\partial\hat{C}}{\partial x_j}\right) = \frac{\partial\mathcal{A}_{ij}}{\partial x_i}\frac{\partial\hat{C}}{\partial x_j}, \qquad (4.16)$$

which is in effect a convective term. Thus, only the symmetric part $\mathcal{D}_{ij}$ should be identified as the dispersion tensor. Hence Eq. (4.10a) can be rewritten by virtue of the antisymmetry of $\mathcal{A}_{ij}$ as

$$\frac{\partial\hat{C}}{\partial T} + \frac{\partial}{\partial x_i}\left[\left(\mathcal{U}_i + \frac{\partial\mathcal{A}_{ij}}{\partial x_j}\right)\hat{C}\right] = \frac{\partial}{\partial x_i}\left[(\mathcal{D}_{ij} + D\delta_{ij})\frac{\partial\hat{C}}{\partial x_j}\right], \qquad (4.17a)$$

where from (4.10c) and (4.14)

$$\mathcal{D}_{ij} = \frac{\Re(H_4)}{\omega}\Re(U_{0i}^*U_{0j}) \qquad (4.17b)$$

$$\mathcal{A}_{ij} = \frac{\Im(H_4)}{\omega}\Im(U_{0i}^*U_{0j})(\delta_{ij} - 1). \qquad (4.17c)$$

Thus the effective convection velocity is

$$\mathcal{U}_i + \frac{\partial\mathcal{A}_{ij}}{\partial x_j}, \qquad (4.18)$$

which is due in part to Eulerian streaming resulting from correlations of oscillating velocities and in part to $\mathcal{A}_{ij}$ resulting from correlations between oscillating velocity and concentration. Further insight into the property of the tensor $\mathcal{A}_{ij}$ can be gained by considering waves in water of constant depth. It follows from the first-order theory that

$$U_{0i} = -\frac{ig}{\omega\cosh(kh)}\frac{\partial\eta}{\partial x_i}$$

(Mei 1983) so that

$$U_{0i}^*U_{0j} \propto \frac{\partial\eta^*}{\partial x_i}\frac{\partial\eta}{\partial x_j}, \qquad (4.19)$$

where h is the water depth and η is the spatial distribution of the free surface defined by $\zeta = \eta(x, y)e^{-i\omega t}$. Let

$$\eta = A(x, y)e^{i\psi(x,y)}, \qquad (4.20)$$

where both A and ψ are real. Then $\vec{k}_p = \nabla\psi$ is the wavenumber vector associated with a progressive wave component. Using (4.19), we have

$$\mathcal{A}_{ij} \propto \Im(U_{0i}^*U_{oj}) \propto \Im\left(\frac{\partial\eta^*}{\partial x_i}\frac{\partial\eta}{\partial x_j}\right) \propto \frac{\partial A^2}{\partial x_i}k_{pj} - \frac{\partial A^2}{\partial x_j}k_{pi}. \qquad (4.21)$$

If, for example, the propagation is along the x axis, then $\vec{k}_p = (k_p, 0)$ and

$$\mathcal{A}_{ij} \propto \frac{\partial A^2}{\partial y}k_p\epsilon_{3ji}, \qquad (4.22)$$

where ϵ_{3ji} is the permutation symbol. Thus, the tensor $\mathcal{A}_{ij}$ exists only if the wave field has a progressive component ($\nabla\psi \neq 0$) and an energy gradient transverse to the direction of propagation. This conclusion holds locally if $\vec{k}_p$ is a function of space. In particular, for either a pure standing wave (ψ = constant) or a long-crested progressive wave (no lateral gradient of energy), $\mathcal{A}_{ij} = 0$. Further, we see in the case of k_p = constant that the additional convection is

$$\frac{\partial\mathcal{A}_{ij}}{\partial x_j} \propto \frac{\partial}{\partial x_j}\left(\frac{\partial A^2}{\partial y}\right)k_p\epsilon_{3ji}. \qquad (4.23)$$

Thus, the gradient of the energy gradient normal to the direction of the propagating wave component generates a transverse convective velocity. This velocity is weaker if the progressive wave is longer.

c. *Effects of particle size and wave pattern*

First we note that the smaller the particles, the smaller the parameter $\mathrm{Pe} = \delta/d = w_0\delta/D$. The physical implications of the effect of Pe on dispersion are easiest to see for long-crested waves propagating in the x direction only, in which case the only nonzero component in $\mathcal{D}_{ij}$ is $\mathcal{D}_{xx}/(U_0^2/\omega) = \Re(H_4)$. We see from Fig. 1c that the coefficient $\Re(H_4)$ is the greatest near Pe = O(1) for all Sc and diminishes for either large or small Pe. Thus, the longitudinal dispersion is relatively small for either large or small Pe. This is reasonable since for a fixed oscillatory boundary layer thickness δ, d increases with decreasing particle size. Smaller particles with $\mathrm{Pe} \ll 1$ do not tend to crowd near the bottom of the boundary layer where the shear rate is high, hence the longitudinal dispersion is small, as explained by Sumer (1974) for steady flows. On the other hand, when $\delta/d \gg 1$, most of the heavy particles are concentrated close to the bottom where the velocity is nearly zero. In the limit $d/\delta \to 0$, all particles are stuck on the bottom; longitudinal dispersion must also be small, as also noted by Yasuda (1989).

The effects of wave pattern (through U_0 and V_0) on convection velocity and dispersion are best examined for specific examples as in the next sections. To help understand later results we discuss here the special case of dispersion in a one-dimensional pure standing wave. Since $U_0 = 0$ beneath an antinode, $\mathcal{D}_{xx}$ and $\mathcal{U}$ vanish

TABLE 1. The Peclét number $Pe = w_0\delta/D$.

	$2a$ (m)	
ω (rad s^{-1})	10^{-4}	10^{-5}
0.5	1.4	0.014
0.02	10	0.1

there by (4.11) and (4.17b). With $\Re(H_1) < 0$ and $\Re(H_4) > 0$, we have at the same point

$$\frac{\partial \mathcal{U}}{\partial x} \propto -\frac{\partial^2 |U_0|^2}{\partial x^2} \propto -\frac{\partial^2 \mathcal{D}_{xx}}{\partial x^2} < 0;$$

hence $\mathcal{U}$ must be positive on the left and negative on the right of the antinode. It follows that $\mathcal{U}$ converges toward the antinode. This is consistent with the known fact that in a standing wave the horizontal Eulerian streaming throughout most of the boundary layer depth except very near the bottom converges to the antinodes (Mei 1983). A particle cloud, wherever it may be initially, must be transported mostly toward the nearest antinode. Note in Fig. 1a that there is a range of very large Pe (heavy or large particles) where $\Re(H_1) > 0$; the mean convection velocity $\mathcal{U}_i$ reverses sign. This is because (i) $\mathcal{U}_i$ is depth-integrated with the weight F, which is significant only in a very thin layer near the seabed if the fall velocity is relatively large, and (ii) near the bed the Eulerian streaming converges toward the nodes and diverges away from the antinodes (see Mei 1983). Thus, for relatively heavy particles, convection tends to inhibit the cloud from diffusing toward the antinode. This range of Pe is, however, very small where other physical effects neglected here may complicate the present theory.

To have some quantitative ideas of the practical range of the parameter Pe, we use the Stokes formula for a sphere of radius a,

$$w_0 = \frac{2ga^2}{9\nu}\left(\frac{\rho_s - \rho}{\rho}\right), \tag{4.24}$$

to estimate the fall velocity. For a fine quartz particle or silt in water at 20°C, $w_0 \sim 0.9 \times 10^4 (2a)^2$, where w_0 is in centimeters per second and a in centimeters. In a wave tank of artificially roughened bottom, Jonsson and Carlsen (1976) conducted wave experiments where the orbital velocity U_0 is in the range 147 ~ 220 cm s^{-1} and orbital amplitude A is 179 ~ 285 cm. From the turbulence-average velocity profiles they found the eddy viscosity to be as high as 100 cm^2 s^{-1} in the boundary layer. Let us take half this value for estimation $\nu_e = 0.005$ m^2 s^{-1}. [An alternate estimate based on the semi-empirical theories of Kajiura (1968) and Grant and Madsen (1979) yields similar order of magnitude.] Also, we choose two frequencies with $\omega = 0.5$ rad s^{-1} typical of surface gravity waves and $\omega = 0.02$ rad s^{-1} typical of internal gravity waves. Table 1 lists the sample values of Pe for two particle diameters. It can be seen that in these combinations of ν_e and ω, Pe can assume a wide range of values, and for both surface and internal waves there is a range of particle sizes that correspond to Pe = O(1) where the dispersion coefficient is the largest.

d. Comparison of dispersivity and diffusivity

Equations (4.17a–c) may be normalized by defining $\bar{U}_0$ to be the maximum of the first-order velocity $(U_0^2 + V_0^2)^{1/2}$ and letting

$$U'_{0_i} = \frac{U_{0_i}}{\bar{U}_0}, \quad x'_i = kx_i, \quad t' = \frac{k^2 \bar{U}_0^2}{\omega} T, \tag{4.25}$$

where primes denote dimensionless quantities. Then

$$\frac{\partial \hat{C}}{\partial t'} + \frac{\partial}{\partial x'_i}\left[\left(\mathcal{U}'_i + \frac{\partial \mathcal{A}'_{ij}}{\partial x'_j}\right)\hat{C}\right] = \frac{\partial}{\partial x'_i}\left(K'_{ij}\frac{\partial \hat{C}}{\partial x'_j}\right), \tag{4.26}$$

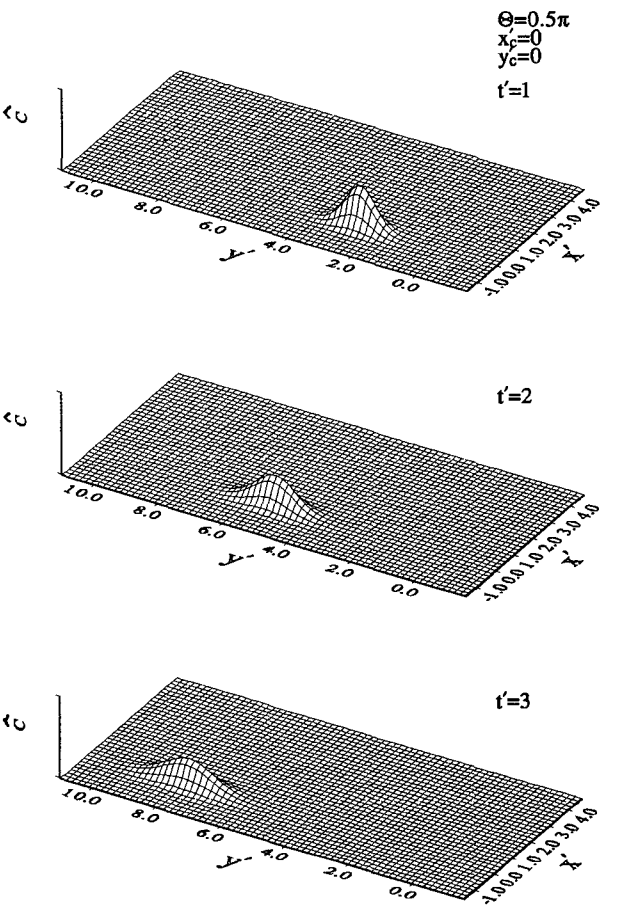

FIG. 2. Evolution of an initially Gaussian cloud with variance $\sigma'^2 = 0.05$ in a progressive wave along the y' axis ($\theta = \pi/2$).

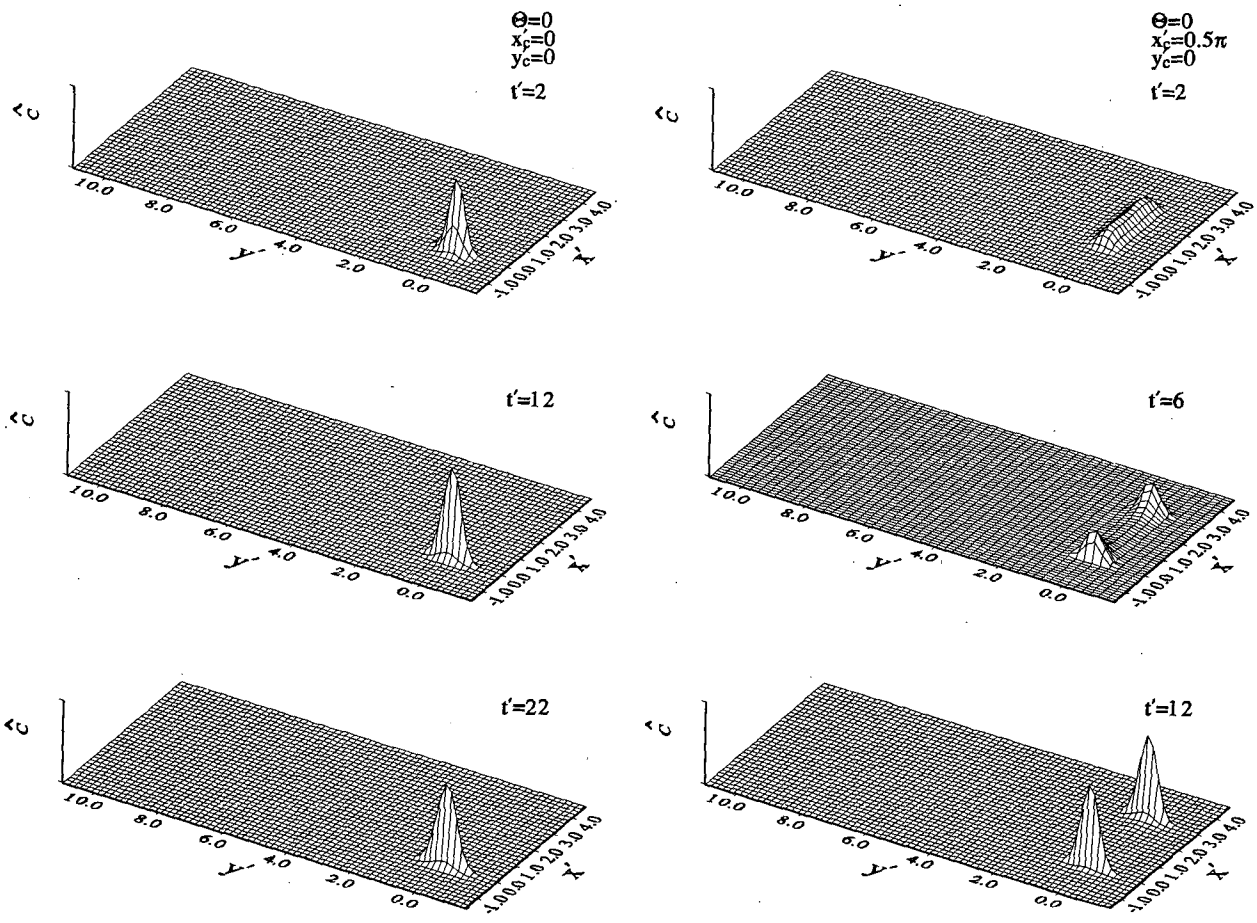

FIG. 3. The same initial cloud as in Fig. 2 in a pure standing wave ($\theta = 0$) with $y_c' = 0$ and x_c' at (a) 0, (b) $\pi/2$, and (c) $\pi/4$.

where

$$\mathcal{U}_i' = \mathcal{U} \Big/ \frac{\kappa \bar{U}_0^2}{\omega} \tag{4.27a}$$

$$K_{ij}' = (\mathcal{D}_{ij}' + D'\delta_{ij}) \tag{4.27b}$$

$$(\mathcal{D}_{ij}', D') = (\mathcal{D}_{ij}, D)/(\bar{U}_0^2/\omega). \tag{4.27c}$$

For practical estimates of the relative magnitudes of $\mathcal{D}_{ij}'$ and D', we note that, in steady channel or tube flows the longitudinal dispersion coefficient is much greater than the eddy diffusivity. To see whether this is true in the oscillatory boundary layer here, we estimate again from the measurements of Jonsson and Carlson (1976) for an artificially roughened bed that the representative eddy viscosity is $\nu_e = 50\ \text{cm}^2\ \text{s}^{-1} = 0.005\ \text{m}^2\ \text{s}^{-1}$. The order of magnitude of $\mathcal{D}_{ij}$ is $(\Re H_1)U^2/\omega$. From Fig. 1c the largest value of $\Re(H_4)$ is about 2.4×10^{-2} occurring at Pe ≈ 1. If we take $U = 1\ \text{m s}^{-1}$ and $\omega = 2\pi/10$ (period = 10 sec) corresponding to a swell of medium amplitude, the scale of $\mathcal{D}_{ij}$ is $0.04\ \text{m}^2\ \text{s}^{-1}$, much greater than the eddy viscosity. Being inversely proportional to ω, the dispersion coefficient increases with decreasing frequency (such as internal gravity waves with period = O(100 s); it can hence still be much greater than the eddy diffusivity.

In summary, we emphasize that the spatial variation of the wave field not only enhances diffusion through the dispersion tensor $\mathcal{D}_{ij}$ but also advection through the second term in the combination $\mathcal{U}_i + (\partial \mathcal{A}_{ij}/\partial x_j)$. This dual effect has been emphasized by Geyer and Signal (1992) in their review of tidal dispersion. Our theory is quite general so far since the wave pattern is as yet unspecified. Details can vary significantly through the inviscid free-stream velocity amplitudes U_0, V_0 outside the boundary layer. In general, one may expect that the fate of a cloud of particles depends on its initial size and location, and the variation of $\mathcal{U}$, $\mathcal{V}$, $\mathcal{A}_{ij}$, and $\mathcal{D}_{ij}$ along its path. To gain more insight we shall examine two examples for which the inviscid flow fields are very simple.

5. Two-dimensional diffusion of a localized cloud in bidirectional waves

Consider a system of short-crested waves as a result of a plane wave of amplitude A_0, frequency ω, and

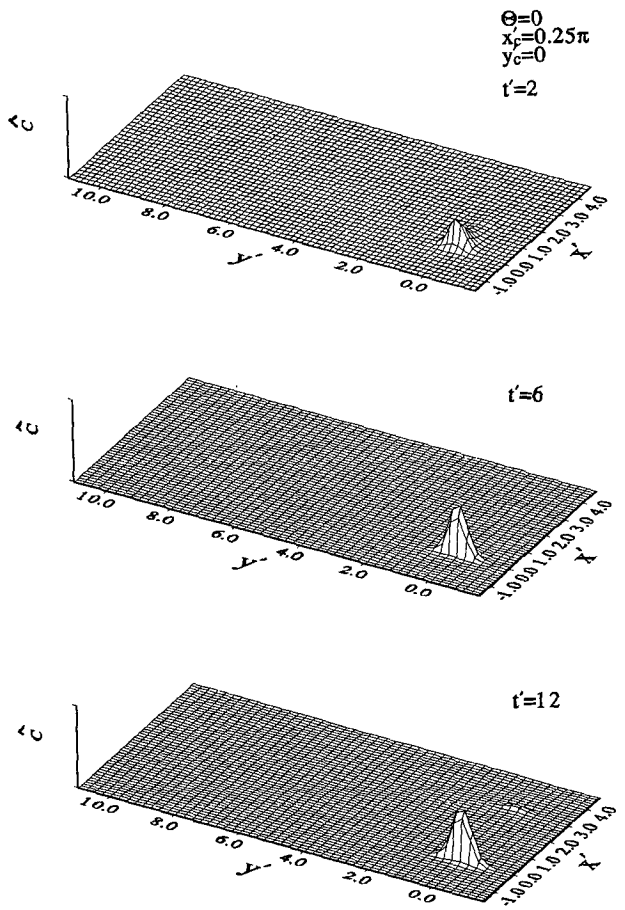

FIG. 3. (*Continued*)

wavenumber k incident at an angle θ from the x axis toward, and reflected by, a sea wall along the y axis. The free surface and the amplitudes of free stream velocities are then given by

$$\zeta = 2A_0 \cos(k\cos\theta x)e^{i(k\sin\theta y-\omega t)} \tag{5.1}$$

and

$$U_0 = 2i\bar{U}_0 \cos\theta \sin(k\cos\theta x)e^{ik\sin\theta y},$$

$$V_0 = 2\bar{U}_0 \sin\theta \cos(k\cos\theta x)e^{ik\sin\theta y}, \tag{5.2}$$

where $\bar{U}_0 = \sqrt{U_0^2 + V_0^2}$. Normalized according to (4.25), the coefficients in the dispersion equation (4.26) read

$$\mathcal{U}' = [2\Re(H_1)\cos^3\theta + (\Re(H_3) - \Re(H_2)) \times \sin\theta \sin(2\theta)]\sin(2x'\cos\theta)$$

$$\mathcal{V}' = [2\Im(H_1)\sin^3\theta + \Im(H_3)\cos\theta\sin(2\theta)]2\cos^2(x'\cos\theta)$$

$$\mathcal{D}'_{xx} = 4\Re(H_4)\cos^2\theta\sin^2(x'\cos\theta)$$

$$\mathcal{D}'_{yy} = 4\Re(H_4)\sin^2\theta\cos^2(x'\cos\theta)$$

$$\mathcal{D}'_{xy} = \mathcal{D}'_{yx} = 0$$

$$\mathcal{A}'_{xy} = -\mathcal{A}'_{yx} = \Im(H_4)\sin(2\theta)\sin(2x'\cos\theta)$$

$$\frac{\partial \mathcal{A}'_{xy}}{\partial y'} = 0,$$

$$\frac{\partial \mathcal{A}'_{yx}}{\partial x'} = 2\Im(H_4)\sin(2\theta)\cos\theta\cos(2x'\cos\theta). \tag{5.3}$$

Note that, from (5.1), the free surface amplitude and phase functions as defined in (4.20) are

$$A(x) = 2A_0\cos(k\cos\theta x)$$

$$\psi(y) = k\sin\theta y. \tag{5.4}$$

Therefore, there is a progressive wave propagating in the y direction with $\vec{k}_p = (0, k\sin\theta)$, while the gradient of the cross-wave energy gradient exists only in the x direction. Hence, the additional convection is present in the y direction only, agreeing with the more general comments made in the previous section. Also evident is that, when $\theta = 0$ (standing wave) or $\theta = \pi/2$ (pure progressive wave along the wall), $\vec{k}_p = 0$ or $A = \text{const}$; in either case the tensor $\mathcal{A}_{ij}$ vanishes.

Let us examine the dispersion pattern involving the combined effects of coefficients in (5.3) of an impulsively released Gaussian cloud centered at x'_c, y'_c with a variance $\sigma'^2 = 0.05$. Assuming $\text{Sc} = M = 1$, we have $\Re(H_1) = -0.122$, $\Im(H_1) = \Im(H_3) = 0.659$, $\Re(H_2) = 0.033$, $\Re(H_3) = -0.155$, $\Re(H_4) = 0.024$, and $\Im(H_4) = 0.234$. Choosing $D' = 10^{-3}$, the initial value problem is solved numerically by a Peaceman-Rachford ADI (alternating direction) finite-difference method. Three angles of incidence and various positions of the initial source center have been considered.

For a plane progressive wave propagating along the sea wall (the y axis) $\theta = \pi/2$, so only $\mathcal{V}'$ and $\mathcal{D}'_{yy}$ are nonzero by (5.3) and are constants. As shown in Fig. 2, the cloud is simply convected along the direction of wave propagation and becomes increasingly elongated in y since $\mathcal{D}'_{yy}/D' = 24$.

For a plane standing wave corresponding to normal incidence toward the sea wall, $\theta = 0$. The nonzero coefficients are $\mathcal{U}'$ and $\mathcal{D}'_{xx}$, both being functions of x'. Since now $\mathcal{D}'_{xx}/D' = 24$, dispersion in x' dominates. The spatial dependencies of $\mathcal{U}'$ and $\mathcal{D}'_{xx}$ cause the pattern of spreading to depend on the location of release. Indeed, if the initial cloud is located at $x'_c = 0$, $y'_c = 0$ where there is no convection and dispersion is the weakest, the peak does not move but the rest of cloud is convected inward. Hence the distribution becomes more and more localized as shown in Fig. 3a. On the other hand, if $x'_c = \pi/2$ (Fig. 3b), $\mathcal{U}'$ diverges away so the initial pulse is split in two toward $x' = 0$ and π, where the convection velocity converges and the dispersion is weak. For $x'_c = \pi/4$, most of the cloud is slanted by convection toward $x' = 0$; only a small part is transported to $x' = \pi$, see Fig. 3c.

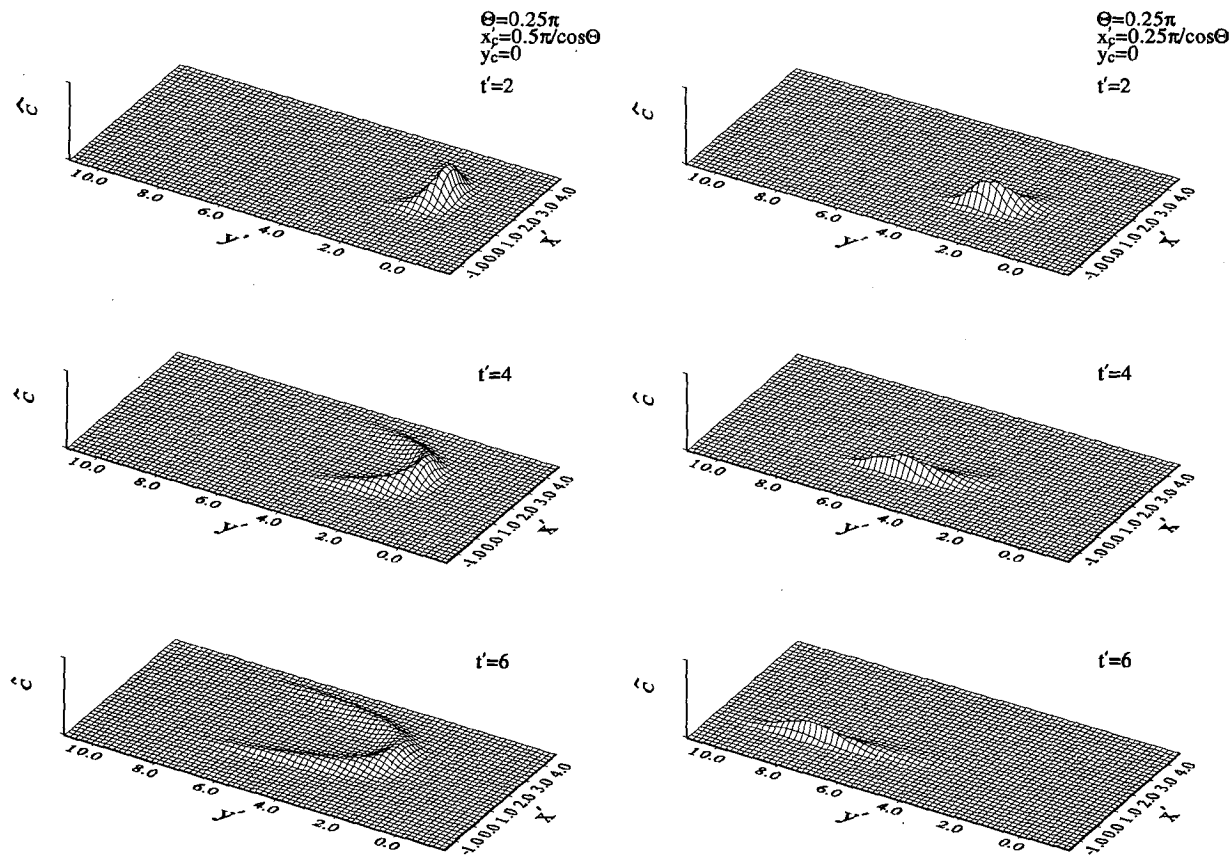

FIG. 4. The same initial cloud as in Fig. 2 in a plane wave incident at $\theta = \pi/2$ with $y_c' = 0$ and $x_c' \cos\theta$ at (a) $\pi/2$ and (b) $\pi/4$.

Finally, for oblique incidence $\theta = \pi/4$, all nonzero coefficients in (5.3) appear and are functions of x'. For $x_c' = 0$ where dispersion and convection vanish in x' but are the greatest in y', the result is similar to Fig. 2 except that the convection speed in y' is lower since $\mathcal{V}'$ is now a projected component and the additional convection is in the opposite direction as can be shown from (5.3). For $x_c' \cos\theta = \pi/2$, the nonuniform convection velocity causes the cloud to bifurcate toward the lines $x_c' \cos\theta = 0$ and π where stronger dispersion and convection in y' take over, as shown in Fig. 4a. When $x_c' \cos\theta = \pi/4$, most of the pulse is convected to the left, with the front leading the rest in the shape of an eel, as shown in Fig. 4b.

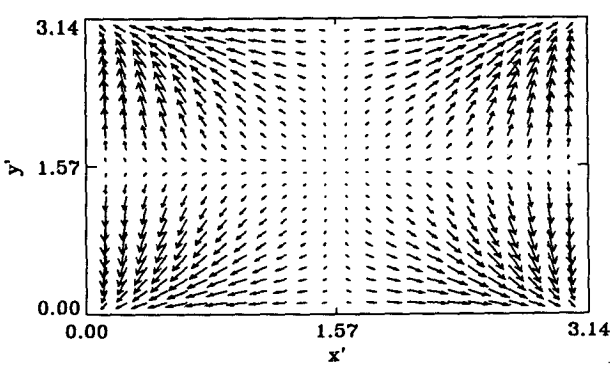

FIG. 5. Convection velocity field in a seiching lake of aspect ratio $s = b/a = 0.5$. In the figure, x' and y' are normalized, respectively, by a/π and b/π.

6. Two-dimensional dispersion in a seiching lake

Let us examine the dispersion in the bottom boundary layer beneath a standing wave in a rectangular lake. Let the basin have the depth h, width a, and length b. The free surface displacement of the seiche mode is assumed to be

$$\zeta = A_0 \cos\frac{\pi x}{a} \cos\frac{\pi y}{b} e^{-i\omega t}, \tag{6.1}$$

where A_0 is a constant. The amplitudes of the free stream velocities are then given by

$$U_0 = \frac{i\pi g A_0}{a\omega} \frac{1}{\cosh kh} \sin\frac{\pi x}{a} \cos\frac{\pi y}{b}$$

$$V_0 = \frac{i\pi g A_0}{b\omega} \frac{1}{\cosh kh} \cos\frac{\pi x}{a} \sin\frac{\pi y}{b}. \tag{6.2}$$

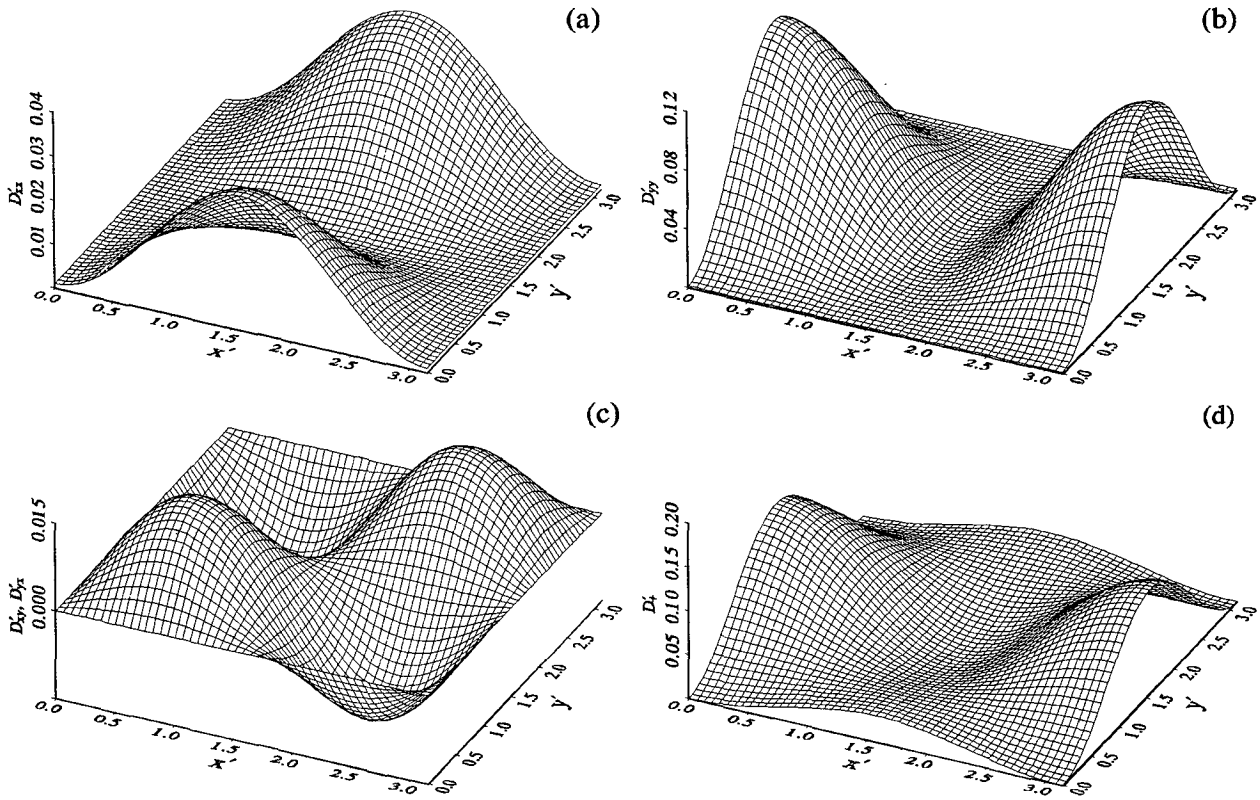

FIG. 6. Distributions of the components of the induced dispersivity tensor $\mathcal{D}'_{ij}$ in the lake (a, b, c) and that of the principal component $\mathcal{D}'_{+}$ of the diagonalized dispersivity tensor (d).

For internal gravity waves, only the coefficients of U_0 and V_0 are different. Using

$$\bar{U}_0 = \frac{\pi g A_0}{\omega} \frac{1}{\sqrt{a^2 + b^2}} \frac{1}{\cosh kh} \tag{6.3}$$

to normalize the velocity components and $(a/\pi, b/\pi)$ to normalize (x, y), we get in dimensionless form

$$U'_0 = i\sqrt{1 + s^2}\,\sin x' \cos y',$$
$$V'_0 = i\sqrt{1 + s^{-2}}\,\cos x' \sin y', \tag{6.4}$$

where s denotes the aspect ratio,

$$s \equiv \frac{b}{a}. \tag{6.5}$$

The resulting coefficients are, in dimensionless form,

$$\mathcal{U}' = \tfrac{1}{2}\,\Re[((1 + s^2)H_1 + (s + s^{-1})H_3) \times \cos^2 y' - (s + s^{-1})H_2 \sin^2 y']\sin 2x'$$
$$\mathcal{V}' = \tfrac{1}{2}\,\Re[((1 + s^{-2})H_1 + (s + s^{-1})H_3)\cos^2 x' - (s + s^{-1})H_2 \sin^2 x']\sin 2y'. \tag{6.6}$$

In this case A'_{ij} vanishes since the tensor $U'^{*}_{0i} U'_{0j}$ is real, and

$$\mathcal{D}'_{xx} = \Re(H_4)(1 + s^2)\sin^2 x' \cos^2 y' + D'$$
$$\mathcal{D}'_{yy} = \Re(H_4)(1 + s^{-2})\cos^2 x' \sin^2 y' + D'$$
$$\mathcal{D}'_{xy} = \mathcal{D}'_{yx} = \tfrac{1}{4}\,\Re(H_4)(s + s^{-1})\sin 2x' \sin 2y'. \tag{6.7}$$

The fields of the horizontal convection velocity and the dispersivity tensor $\mathcal{D}'_{ij}$ are shown in Figs. 5 and 6a–c, respectively. Note the horizontal convergence toward the corners, suggesting upwelling there. The total dispersivity tensor $K'_{ij} = \mathcal{D}'_{ij} + D'\delta_{ij}$ can be easily diagonalized as follows. Let λ be the eigenvalues defined by

$$|K'_{ij} - \lambda\delta_{ij}| = 0, \tag{6.8}$$

then

$$\begin{pmatrix}\lambda_+ \\ \lambda_-\end{pmatrix} = \tfrac{1}{2}\,[K'_{xx} + K'_{yy} \pm \sqrt{(K'_{xx} + K'_{yy})^2 - 4(K'_{xx}K'_{yy} - K'_{xy}K'_{yx})}]. \tag{6.9}$$

The eigenvectors (α_+, β_+) and (α_-, β_-) are orthogonal and represent the major $(+)$ and minor $(-)$ axes, respectively, whose inclinations with the x axis are

$$\tan\theta_\pm = \frac{\beta_\pm}{\alpha_\pm} = -\frac{K'_{xx} + K'_{yx} - \lambda_\pm}{K'_{yy} + K'_{xy} - \lambda_\pm}. \tag{6.10}$$

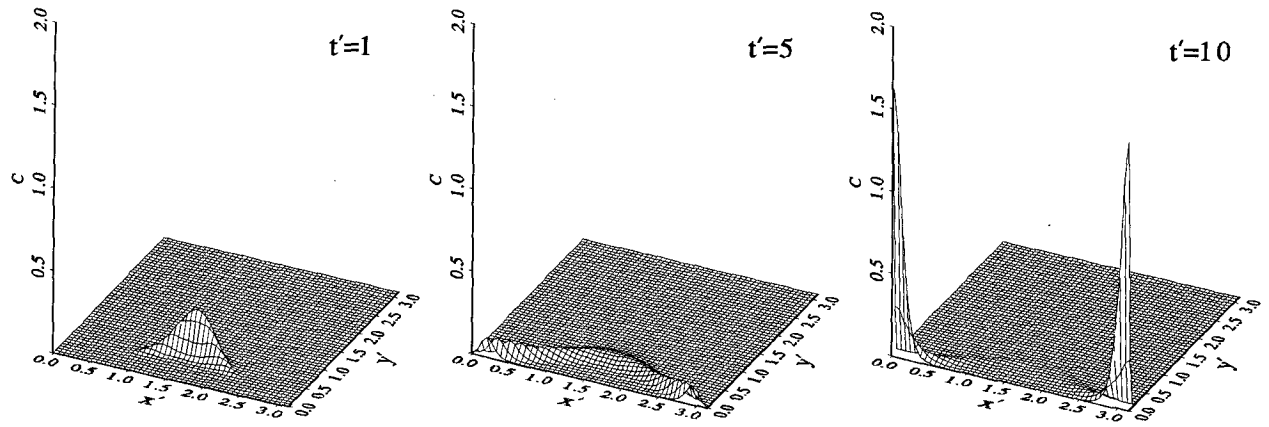

FIG. 7. Dispersion of a cloud (as in Fig. 2 initially) released at x'_c, $y'_c = \pi/2, \pi/4$ in a seiching lake of aspect ratio $s = 0.5$.

In the rectilinear coordinate system formed by these axes, the dispersion tensor is diagonal with only two nonzero components $K'_+ = \lambda_+$ and $K'_- = \lambda_-$. Substituting (6.7) into (6.10), we get

$$\tan\theta_\pm = \frac{1}{s}\frac{\tan y'}{\tan x'} \tag{6.11}$$

and

$$K'_\pm = D' + \mathcal{D}'_\pm \tag{6.12}$$

with

$$\mathcal{D}'_+ = \Re(H_4)[(1+s^2)(\sin x'\cos x')^2 + (1+s^{-2})(\cos x'\sin y')^2] \tag{6.12a}$$

$$\mathcal{D}'_- = 0. \tag{6.12b}$$

We plot the convection velocity field in Fig. 5 and the distribution of the coefficient $\mathcal{D}'_+$ in Fig. 6d. For $s = 1/2$, the orientation of the major axis varies in space in approximately the same way as the convection velocity as shown in Fig. 5. In particular, $\theta_+ = 0$ along the north–south axis of the lake ($x' = \pi/2$) and along the north and south coasts ($y' = 0, \pi$), $\theta_+ = \pi/2$ along the east–west axis ($y' = \pi/2$) and the east and west coasts ($x' = 0, \pi$). Thus, the shear-induced dispersivity $\mathcal{D}'_+$ enhances spreading along the coast. For a square lake, $s = 1$, the principal direction of a dispersion tensor along the diagonal follows the diagonal. We now present sample numerical results for the release of a Gaussian cloud of unit height with $\sigma'^2 = 0.05$. The dimensionless eddy diffusivity is taken to be $D' = 10^{-3}$. Since $U'_0 = 0$ along the lake boundaries, $x' = 0, \pi$; $0 < y' < \pi$, and $V'_0 = 0$ along $y' = 0, \pi$; $0 < x' < \pi$, the no-flux boundary condition $\mathcal{F}_i n_i = 0$ implies

$$\frac{\partial \hat{C}}{\partial x'_i} n_i = 0.$$

Evolution of $\hat{C}$ has been computed for various center locations x'_c, y'_c. In Fig. 7, the initial center is at x'_c, $y'_c = \pi/2, \pi/4$ (south of the lake center). Since $|\theta_+|$ vanishes at the initial center of release and remains small in the region where $\mathcal{D}'_+$ is significant, the cloud is spread mainly in the x direction. Once reaching a

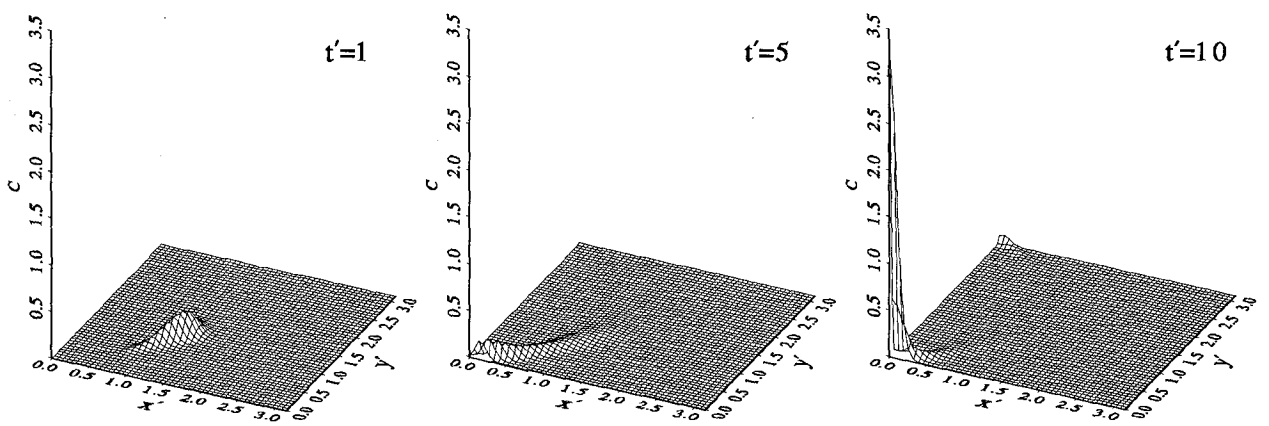

FIG. 8. The same cloud as in Fig. 7 released at x'_c, $y'_c = 3\pi/8, 3\pi/8$.

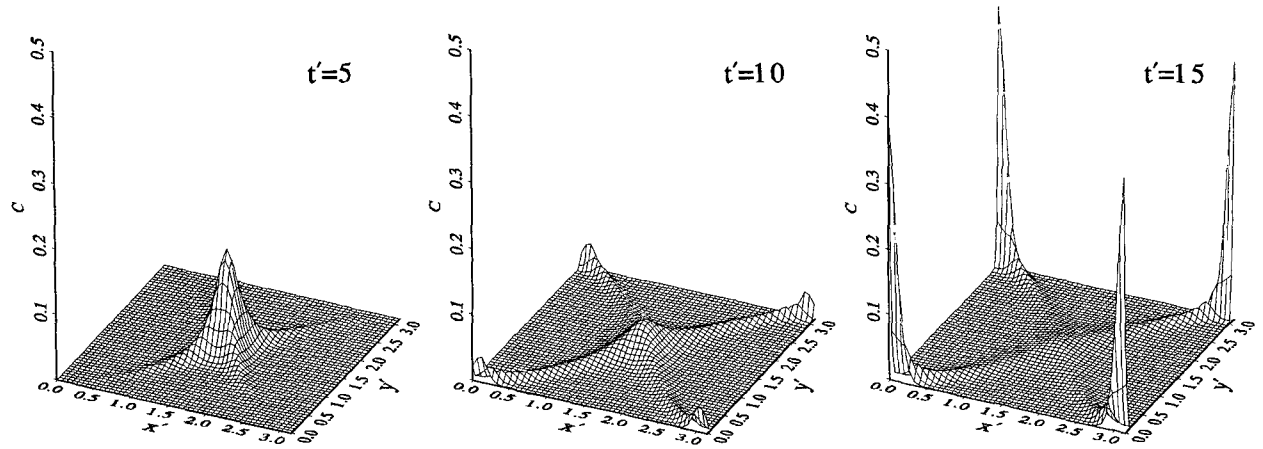

FIG. 9. The same cloud as in Fig. 7 released at x_c', $y_c' = \pi/2, \pi/2$.

diagonal, $|\theta_+|$ approaches $\tan^{-1}(2) \approx 63.4°$ for $s = 1/2$. Dispersion and convection help each other in transporting the cloud toward the two corners at 0, 0 and π, 0 on the south side. If the initial cloud is released at a point west of the lake center, say $(x_c', y_c') = (\pi/4, \pi/2)$, the cloud is split first by dispersion, and then convected and diffused toward the corners on the west side. Since the qualitative features are the same as in the previous case, plots are omitted. For an initial cloud released on a diagonal, the evolution is shown in Fig. 8. Dispersion is directed in the direction $|\theta_+| = 63.4° > 45°$ away from the diagonal along which $\mathcal{D}_+'$ is small, hence convection prevails and brings the cloud back toward the diagonal and then the corner, following a curved path. Finally, if the initial cloud is released at the lake center, it is split into four equal parts, drifting and spreading toward all four corners, as shown in Fig. 9. In all examples, the suspension accumulates at the corner(s) and approaches a steady limit there. This is because at the corners $\mathcal{D}_+'$ vanishes and only D' is effective. Weak outward diffusion through eddy viscosity is balanced by inward convection.

7. Concluding remarks

We have presented a theory of dispersion in a wave boundary layer, with a view to examining the effects of horizontal variation of the wave pattern on the dispersion process. For small amplitude waves, the fluctuating part of the velocity field is much greater than the steady mean; therefore, it is possible to apply a perturbation method and achieve Reynolds averaging without any difficulty in closure. The correlations between concentration and velocity oscillations are calculated explicitly, under the simplifying assumption of constant eddy viscosity and mass diffusivity. It is found that in general, correlation between oscillating velocities, that is, Eulerian streaming, contributes to steady convection, whereas correlation between oscillating fluid velocity and concentration contributes to both dispersion and convection. Examples are discussed for dispersion from a localized cloud under a bidirectional wave or a seiche in a lake. The spreading pattern in general depends strongly on the location of release due to the spatial dependence of the dispersivities and the convection velocity. The cloud tends to accrete at points toward which the Eulerian streaming converges horizontally and where dispersivity is weak.

It should be pointed out that the present model is based on two underlying assumptions: (i) constant eddy diffusivity and (ii) negligible deposition or resuspension. A more realistic turbulence closure model amounting to time-dependent eddy diffusivity and/or erodible bottom may change the results significantly.

In summary, our general theory and specific examples serve to demonstrate that the detailed horizontal variation of convection velocity and dispersion tensor, which depend on the complexity of the wave pattern, must be the crucial part of any pollutant transport model. Indeed a numerical model that depends on empirical estimates of the dispersion tensor cannot be fully reliable if it is calibrated against field measurements at only a few stations. To modify this theory for sediment diffusion over an erodible bed, consideration of resuspension at the bed and more complex modeling of turbulence are necessary. While empirical hypotheses on the bottom boundary condition have been proposed, the real challenge remains to be the better understanding of the physics of resuspension, sediment deposition and entrainment at the seabed.

Acknowledgments. We are grateful for the financial support by the Ocean Engineering Program, U.S. Office of Naval Research Contract N00014-89-J-3128, and the Fluid/Hydraulics/Particulates Program of the U.S. National Science Foundation (Grant CTS-9115689). Comments by Carole Womeldorf, who deduced (4.17c) from (4.14), are appreciated.

APPENDIX

Explicit Formulas for Coefficients H_1, H_2, H_3, H_4

We first recall

$$\mathrm{Pe} = w_0\delta/D = \delta/d \tag{A.1}$$

$$N = \frac{2\sqrt{2\,\mathrm{Sc}}}{\mathrm{Pe}} \tag{A.2}$$

and define the following symbols

$$\begin{pmatrix} A_1 \\ A_2 \end{pmatrix} = -\frac{1}{2}(1 \mp \Gamma_1) \mp \frac{i}{2}\Gamma_2 \tag{A.3}$$

with

$$\begin{pmatrix} \Gamma_1 \\ \Gamma_2 \end{pmatrix} = \left\{\frac{1}{2}10\,[(1+N^4)^{1/2} \pm 1]\right\}^{1/2}. \tag{A.4}$$

It can be shown that

$$\tilde{F}_2 = \int_0^\infty F_2 e^{-\eta} d\eta = \mathrm{Pe}\left[\frac{1-3i}{2(\mathrm{Pe}+1-i)} + \frac{i}{2(\mathrm{Pe}+1+i)} + \frac{1+i}{4(\mathrm{Pe}+2)} - \frac{(1+i)}{2(\mathrm{Pe}+1-i)^2}\right] - \frac{3(1-i)}{4} \tag{A.5}$$

$$\tilde{F}_3 = \int_0^\infty F_3 e^{-\eta} d\eta = \frac{\mathrm{Pe}}{(\mathrm{Pe}+1)^2+1} - \frac{1}{2(\mathrm{Pe}+2)} \tag{A.6}$$

$$\tilde{F}_4 = \int_0^\infty F_4 e^{-\eta} d\eta = \mathrm{Pe}\left[\frac{1-2i}{2(\mathrm{Pe}+1-i)} - \frac{(1+i)}{2(\mathrm{Pe}+1-i)^2} + \frac{i}{4(\mathrm{Pe}+2)}\right] - \frac{2-3i}{4}, \tag{A.7}$$

where $\eta = z/d$. Note that $\tilde{F}_3$ is real. Further,

$$\int_0^\infty \overline{u_1 C_1} dz = \frac{d}{\omega}\Re\left\{B_1 U_0^*\left(U_0\frac{\partial \hat{C}}{\partial x} + V_0\frac{\partial \hat{C}}{\partial y}\right) + B_2 U_0^*\left(\frac{\partial U_0}{\partial x} + \frac{\partial V_0}{\partial y}\right)\hat{C}\right\}, \tag{A.8}$$

where

$$B_1 = \frac{\mathrm{Sc}}{\mathrm{Pe}^2}\left\{\frac{2\,\mathrm{Pe}}{A_2(1+A_2)[1+i-A_2\,\mathrm{Pe}][(1+A_1)\,\mathrm{Pe}+1-i][(1+A_2)\,\mathrm{Pe}+1-i]} + \frac{(1+i)}{[\mathrm{Pe}+1+i](1+A_1)(1+A_2)} - \frac{(1+i)\,\mathrm{Pe}^3}{[\mathrm{Pe}+1-i][(1+A_1)\,\mathrm{Pe}+1-i][(1+A_2)\,\mathrm{Pe}+1-i](2+\mathrm{Pe})}\right\} \tag{A.9}$$

and

$$B_2 = \frac{\mathrm{Sc}}{\mathrm{Pe}^2}\left\{-\frac{(1+i)}{A_2[1+i-A_2\,\mathrm{Pe}]}\left[\frac{\mathrm{Pe}^2}{(1+A_2)[(1+A_1)\,\mathrm{Pe}+1-i][(1+A_2)\,\mathrm{Pe}+1-i]} - \frac{1}{(1+A_2)^2(1+A_1)}\right] + \frac{(2+A_1+A_2)(1+i)-i(1+A_1)(1+A_2)\,\mathrm{Pe}}{[1+i+\mathrm{Pe}](1+A_1)^2(1+A_2)^2} + \frac{i\mathrm{Pe}^4}{[\mathrm{Pe}+1-i](2+\mathrm{Pe})[(1+A_1)\,\mathrm{Pe}+1-i][(1+A_2)\,\mathrm{Pe}+1-i]} + \frac{[1+i+2\,\mathrm{Pe}](1+i)}{[1+i+\mathrm{Pe}]^2(1+A_1)(1+A_2)}\right\}. \tag{A.10}$$

The integral

$$\int_0^\infty \overline{v_1 C_1} dz$$

is of similar form as (A.8) except that U_0^* is replaced by V_0^*. Finally,

$$H_1 = \tilde{F}_2 + B_2^*, \quad H_2 = \tilde{F}_3,$$
$$H_3 = \tilde{F}_4 + B_2^*, \quad H_4 = -B_1. \tag{A.11}$$

Note that H_2 is real and $\Im H_1 = \Im H_3$.

REFERENCES

Aris, R., 1960: On the dispersion of a solute in pulsating flow through a tube. *Proc. Roy. Soc. London,* **A259,** 370–376.

Bagnold, R. A., 1951: The movement of a cohesionless granular bed by fluid flow over it. *Brit. J. Appl. Phys.,* **2,** 29.

Batchelor, G. K., 1965: The motion of small particles in turbulent flow. *Proc. Second Australasian Conf. on Hydraulics and Fluid Mechanics,* Sydney, Australia, 19–41.

Bensoussan, A., J. Lions, and G. Papanicolaou, 1978: *Asymptotic Analysis for Periodic Structures.* North Holland, 700 pp.

Bowden, K. F., 1965: Horizontal mixing in the sea due to a shearing current. *J. Fluid Mech.,* **21,** 83–95.

Chatwin, P. C., 1975: On the longitudinal dispersion of passive contaminant in oscillatory flows in tubes. *J. Fluid Mech.,* **71,** 513–527.

Chian, C., 1993: Dispersion of heavy particles in water waves. Engineer's thesis, Dept. of Civil and Environmental Engineering, Massachusetts Institute of Technology, 140 pp.

Denny, M. W., 1988: *Biology and Mechanics of the Wave-swept Environment.* Princeton University Press, 329 pp.

Dill, L. H., and H. Brenner, 1982: A general theory of Taylor dispersion phenomena. V. Time-periodic convection. *Phys. Chem. Hydrodyn.,* **3,** 267–292.

Fukuoka, S., 1974: A laboratory study on longitudinal dispersion in alternating shear flows. Research Bulletin No. 112, Dept. of Engineering, James Cook University of North Queensland, Australia, 43 pp.

Geyer, W. R., and R. P. Signal, 1992: A reassessment of the role of tidal dispersion in estuaries and bays. *Estuaries,* **15,** 97–108.

Grant, W. D., and O. S. Madsen, 1979: Combined waves and current interactions with a rough bottom. *J. Geophys. Res.,* **84**(C4), 1797–1808.

Holly, E. R., D. R. F. Harleman, and H. B. Fischer, 1970: Dispersion in homogeneous estuary flow. *J. Hydraul. Eng. Div., ASCE,* **96,** 1691–1709.

Hunt, J. N., and B. Johns, 1963: Currents induced by tides and gravity waves. *Tellus,* **15,** 4.

Johns, B., 1970: On the mass transport induced by oscillatory flow in a turbulent boundary layer. *J. Fluid Mech.,* **43,** 177–185.

Jonsson, I. G., and N. A. Carlsen, 1976: Experimental and theoretical investigation in an oscillatory turbulent boundary layer. *J. Hydraul. Res.,* **14**(1), 45.

Kajiura, K., 1968: A model of the bottom boundary layer in water waves. *Bull. Earthquake Res. Inst., Univ. Tokyo,* **146,** 75–123.

Kerssens, P. J. M., L. C. Van Rijn, and N. J. van Wijngaarden, 1977: Model for nonsteady suspended sediment transport. *17th Congr. Int. Assoc. Hydraul. Res.,* Baden-Baden, Germany, 113–120.

Longuet-Higgins, M. S., 1953: Mass transport in water waves. *Philos. Trans. R. Soc. London,* **A245,** 535–581.

——, 1958: The mechanics of the boundary layer near the bottom in a progressive wave. *Proc. Sixth Int. Conf. on Coastal Engineering,* Gainesville, FL, 184–193.

Lumley, J. L., 1978: Two-phase and non-Newtonian flows. *Turbulence,* P. Bradshaw, Ed., Springer-Verlag, 289–324.

Lundgren, H., 1972: Turbulent currents in the presence of waves. *Proc. 13th Int. Conf. on Coastal Engineering,* 623–634.

Mauri, R., 1991: Dispersion, convection and reaction in porous media. *Phys. Fluids,* **A3,** 743–756.

Mei, C. C., 1983: *The Applied Dynamics of Ocean Surface Waves.* Wiley-Interscience, 740 pp.

——, 1991: Heat dispersion in periodic porous media by homogenization method. *Symp. on Multiphase Transport,* ASME, R. Eaton, Ed., 11–16.

——, 1992: Method of homogenization applied to dispersion in porous media. *Transport in Porous Media,* **9,** 261–274.

Noh, Y., and H. J. S. Fernando, 1991: Dispersion of suspended particles in turbulent flow. *Phys. Fluids A,* **3**(7), 1730–1740.

Pedley, T. J., and R. D. Kamm, 1988: The effect of secondary motion on axial transport in oscillatory tube flow. *J. Fluid Mech.,* **193,** 347–367.

Rubinstein, J., and R. Mauri, 1986: Dispersion and convection in periodic porous media. *SIAM J. Applied Math.,* **46,** 1018–1023.

Saffman, P. G., 1962: On the stability of laminar flow of a dusty gas. *J. Fluid Mech.,* **13,** 120–128.

Sayre, W. W., 1968: Dispersion of mass in open-channel flow. Colorado State Univ. Hydraul. Paper No. 3, 73 pp.

——, 1969: Dispersion of silt particles in open-channel flow. *J. Hydraul. Div., ASCE,* **HY3,** 1009–1038.

Shapiro, M., and H. Brenner, 1988: Dispersion of a chemically reactive solute in a spatially periodic model of a porous medium. *Chem. Eng. Sci.,* **43,** 551–571.

Sharp, M. K., R. K. Kamm, A. H. Shapiro, E. Kimmel, and G. E. Karniadakis, 1991: Dispersion in a curved tube during oscillatory flow. *J. Fluid Mech.,* **223,** 537–563.

Sleath, J. F. A., 1990: Seabed boundary layers. *The Sea,* Vol. 9B, B. LeMehaute and D. M. Hanes, Eds., Wiley-Interscience, 693–727.

Smith, J. D., 1977: Modeling of sediment transport on continental shelves. *The Sea,* Vol. 6, E. D. Goldberg, Ed., John Wiley, 539–578.

Smith, R., 1982: Contaminant dispersion in oscillatory flows. *J. Fluid Mech.,* **114,** 379–398.

Staub, C., I. G. Jonsson, and I. A. Svendsen, 1984: Variation of suspended sediments in oscillatory flow. *Proc. 19th Int. Conf. on Coastal Engineering,* Houston, TX, ASCE, 2310–2321.

Sumer, B. M., 1974: Mean velocity and longitudinal dispersion of heavy particles in turbulent open-channel flows. *J. Fluid Mech.,* **65,** 11–28.

Taylor, G. I., 1953: Dispersion of solute matter in solvent flowing slowly through a tube. *Proc. R. Soc. London,* **A219,** 186–203.

Trowbridge, J., and O. S. Madsen, 1984: Turbulent wave boundary layers. 2: Second-order theory and mass transport. *J. Geophys. Res.,* **89**(C5), 7999–8007.

Watson, E. J., 1983: Diffusion in oscillatory pipe flow. *J. Fluid Mech.,* **133,** 233–244.

Yasuda, H., 1989: Longitudinal dispersion of suspended particles in oscillatory currents. *J. Mar. Res.,* **47,** 153–168.

Zimmerman, J. T. F., 1986: The tidal whirlpool: A review of horizontal dispersion by tidal and residual currents. *Neth. J. Sea. Res.,* **30,** 133–154.